Available online at www.sciencedirect.com

SciVerse ScienceDirect

Ceramics International 39 (2013) 3971–3977

CERAMICS INTERNATIONAL

www.elsevier.com/locate/ceramint

Thermodynamic calculations on the chemical vapor deposition of Si–C–N from the $SiCl_4$–NH_3–C_3H_6–H_2–Ar system

Xiaofei Liu, Litong Zhang, Yongsheng Liu*, Fang Ye, Xiaowei Yin

Science and Technology on Thermostructure Composite Materials Laboratory, Northwestern Polytechnical University, Xi'an, Shaanxi 710072, China

Received 7 September 2012; received in revised form 2 October 2012; accepted 23 October 2012
Available online 30 October 2012

Abstract

Based on the Gibbs free energy minimum principle and Factsage software, the thermodynamic phase diagram for the $SiCl_4$–NH_3–C_3H_6–H_2–Ar system was calculated. The effects of temperature, dilution ratio of H_2, total pressure on product types and distribution regions of reacted solid products were discussed. The results show that: (1) The area of SiC–Si_3N_4 increases at first, then decreases with the rising of temperature and reaches the maximum value at 1273.15 K. (2) The ratio of C/Si is the main factor for the deposition of SiC in the double phase of SiC–Si_3N_4. (3) The preferred deposition conditions of Si_3N_4 are: $T=1173.15$ K, H_2:$SiCl_4=10$:1, and $P_{Total}=0.01$ atm. Taking the deposition of SiC into consideration, the deposition of Si_3N_4 influences the formation of Si–C–N directly. (4) According to the influencing factors of depositing SiC and Si_3N_4, the suitable parameter for Si–C–N deposition can be determined. (5) Through the experimental verification, it can be demonstrated that Si–C–N can be obtained by low-pressure chemical vapor deposition (CVD), its product being amorphous and mainly constituted by Si–N and Si–C bonds. The obtained Si–C–N ceramics can transform to α-Si_3N_4 and SiC nano-crystal when heat-treated at 1773.15 K in N_2 for 2 h.

Keywords: $SiCl_4$–NH_3–C_3H_6–H_2–Ar system; Thermodynamic phase diagram; Chemical vapor deposition (CVD)

1. Introduction

In recent years, the deposition of silicon carbon nitride (Si–C–N) has attracted considerable interests due to their attractive properties, such as corrosion resistance, high temperature oxidation resistance, hardness and wide band gap, electronic and other ambient applications [1–6]. At present, the preparation technologies of Si–C–N include pyrolysis of polymer precursors [7], chemical vapor deposition (CVD) at elevated temperatures [8], hot-wire CVD [9], radio frequency plasma-enhanced CVD (PECVD) [10,11], ion beam sputtering [12], hot-pressing process [13] and pulsed high-energy density plasma (PHEDP). Xueming et al. [14] and Nishimura et al. [15] studied mechanical and thermal properties of Si–C–N by pyrolysis of polymer precursors from polyvinylsilazane. This new material was found with excellent properties, but these properties were restrained by the existence of pores accompanied by this method. Izumi and Oda [9] studied the dielectric constant of Si–C–N prepared by HWCVD using Hexamethyldisilazane (HMDS)-NH_3 system. Jedrzejowski et al. studied the mechanical and optical properties of Si–C–N prepared by PECVD with Ar–N_2–SiH_4–CH_4 system. [11] But till now few researches focus on the low-pressure CVD which can reduce some unnecessary reactions and make the deposition well-distributed. Nevertheless the process of low-pressure CVD is very complicated, so thermodynamic calculation of Si–C–N to direct the experiment is necessary.

The thermodynamic calculation can provide informations about the influencing factors of the system, and also it is helpful to predict the extent of reaction and to understand the influence of reaction parameters on the CVD process. From the analysis of the thermodynamic calculation, the deposition mechanism and the optimization of deposition parameters can be well studied. For the $SiCl_4$–NH_3–C_3H_6–H_2–Ar system, there is no associated thermodynamic calculation reported currently.

*Corresponding author. Tel.: +86 029 8849 6068x807; fax: +86 029 8849 4620.
E-mail address: yongshengliu@nwpu.edu.cn (Y. Liu).

0272-8842/$ - see front matter © 2012 Elsevier Ltd and Techna Group S.r.l. All rights reserved.
http://dx.doi.org/10.1016/j.ceramint.2012.10.245

In this paper, the thermodynamic phase diagram and yield map of the CVD process in the $SiCl_4$–NH_3–C_3H_6–H_2–Ar system were calculated within wide ranges of process parameters. The proper parameter was determined. Meanwhile, the principles and mechanisms of the effect of process parameters were discussed.

2. Calculation method

The calculation method is based on the Gibbs free energy minimum principle. First of all, the initial conditions are confirmed, such as system temperature, system total pressure and the dilution ratio of H_2. The temperature range in this passage is from 973.15 K to 1473.15 K; the system total pressures are 0.01 atm, 0.05 atm, 0.1 atm respectively; define $\alpha=[NH_3]/[SiCl_4]$ (N/Si), $\beta=[C_3H_6]/[3SiCl_4]$ (C/Si), ([X] stands for original molar quantity of material X) and both α and β range from 0 to 5. Secondly, all of the thermodynamic calculation datas are from the data base of Factsage software.

The thermodynamic phase diagram and yield map were drawn using the Factsage calculation results to determine the relationship between reaction parameters and product. Because there was no data of Si–C–N in Factsage database, so the data of SiC and Si_3N_4 were used to instead and the focus of Si–C–N is predominantly the double phase SiC–Si_3N_4 accordingly.

3. Results and discussion

3.1. The effect of temperature on the thermodynamic phase diagram and reaction product

Fig. 1 shows the thermodynamic phase diagram with different temperatures from 973.15 K to 1473.15 K. Fig. 2 shows the yield map of SiC–Si_3N_4 in different temperatures from 1173.15 K to 1373.15 K when C/Si=0.6. Temperature plays a key role in both of the formation and yield of SiC–Si_3N_4. The detailed discussions are as follows:

(1) For SiC–Si_3N_4, the double phase field of SiC–Si_3N_4 appears at 1073.15 K and its area increases at first and then decreases with the rising of temperature which reaches the maximum value at 1273.15 K. With the increasing of temperature, the amount of Si_3N_4 is in a down trend [16] which is revealed in Fig. 2. When $SiCl_4$ was utilized as the Si source in the deposition of SiC, the suitable temperature is excess 1273.15 K [17]. Consequently the suitable temperature is 1173.15 K or 1273.15 K, when the pressure is 0.01 atm.
(2) For C–Si_3N_4, the double phase field of C–Si_3N_4 appears at 973.15 K and the area of phase field decreases with temperature. This is chiefly because the deposition of SiC and Si_3N_4 was influenced by temperature.
(3) For Si_3N_4–C–SiC, the three phase field of Si_3N_4–C–SiC appears at 1173.15 K and the changes are similar to C–Si_3N_4.
(4) For C–SiC, the double phase field of C–SiC appears at 1073.15 K and its area increases with temperature. When the temperature exceeds 1273.15 K and C/Si exceeds 1.0, C–SiC is the only phase. Except the influence of temperature, the reaction $Si_3N_4+3C=3SiC+2N_2$ plays an important role.
(5) For SiC and C, the single phase fields of SiC and C appear at 1173.15 K and 1273.15 K respectively, but both of the areas increase with temperature.

Considering the area of SiC–Si_3N_4 and the yield of SiC and Si_3N_4, 1173.15 K is the suitable temperature of Si–C–N deposition.

3.2. The effect of H_2 on the thermodynamic phase diagram and reaction product

Fig. 3 shows the thermodynamic phase diagram with the dilution ratio of H_2 from 5:1 to 20:1 at 1173.15 K. Fig. 4 shows the yield map of SiC–Si_3N_4 with the dilution ratio of H_2 from 0:1 to 20:1 at 1173.15 K when C/Si=0.6. The changes are as follows from Figs. 3 and 4:

(1) For SiC–Si_3N_4, the area of SiC–Si_3N_4 increases firstly and then basically remains unchanged. But they are quite different from the phase diagram without H_2 which is shown in Fig. 1d.
(2) For C–SiC, the area of C–SiC decreases firstly and then remains unchanged.
(3) For other phases, namely SiC, SiC–Si_3N_4–C and C–Si_3N_4, mainly remain unchanged.

It is concluded that the effect of H_2 on promoting the deposition of SiC–Si_3N_4 is obvious but the ratio of H_2 is not the significant factor.

The changes in the diagram can be explained by affinity of chemical reaction and Gas reaction balance theory [18]

$$A = -T\ln\left(J_p/K^{\Phi}\right) \tag{1}$$

$$J_P = \Pi\left(P_B/P^{\Phi}\right)^{V_B} \tag{2}$$

$$mA_{(g)} + nB_{(g)} = xC_{(s)} + yD_{(g)} \tag{3}$$

$$K^{\Phi} = P_D^{y}/\left(P_A^{y} \times P_B^{y}\right) \tag{4}$$

where A is chemical affinity, related to the negative partial derivative of Gibbs energy with respect to extent of reaction at constant pressure and temperature. It is positive for spontaneous reactions. J_P is the product of the partial pressure of the reactants. V_B is negative when corresponding to reactants and positive value when V_B is corresponding to the species. K^{Φ} is equilibrium constant. P_B is the partial pressure of each gas component. P is standard gas pressure.

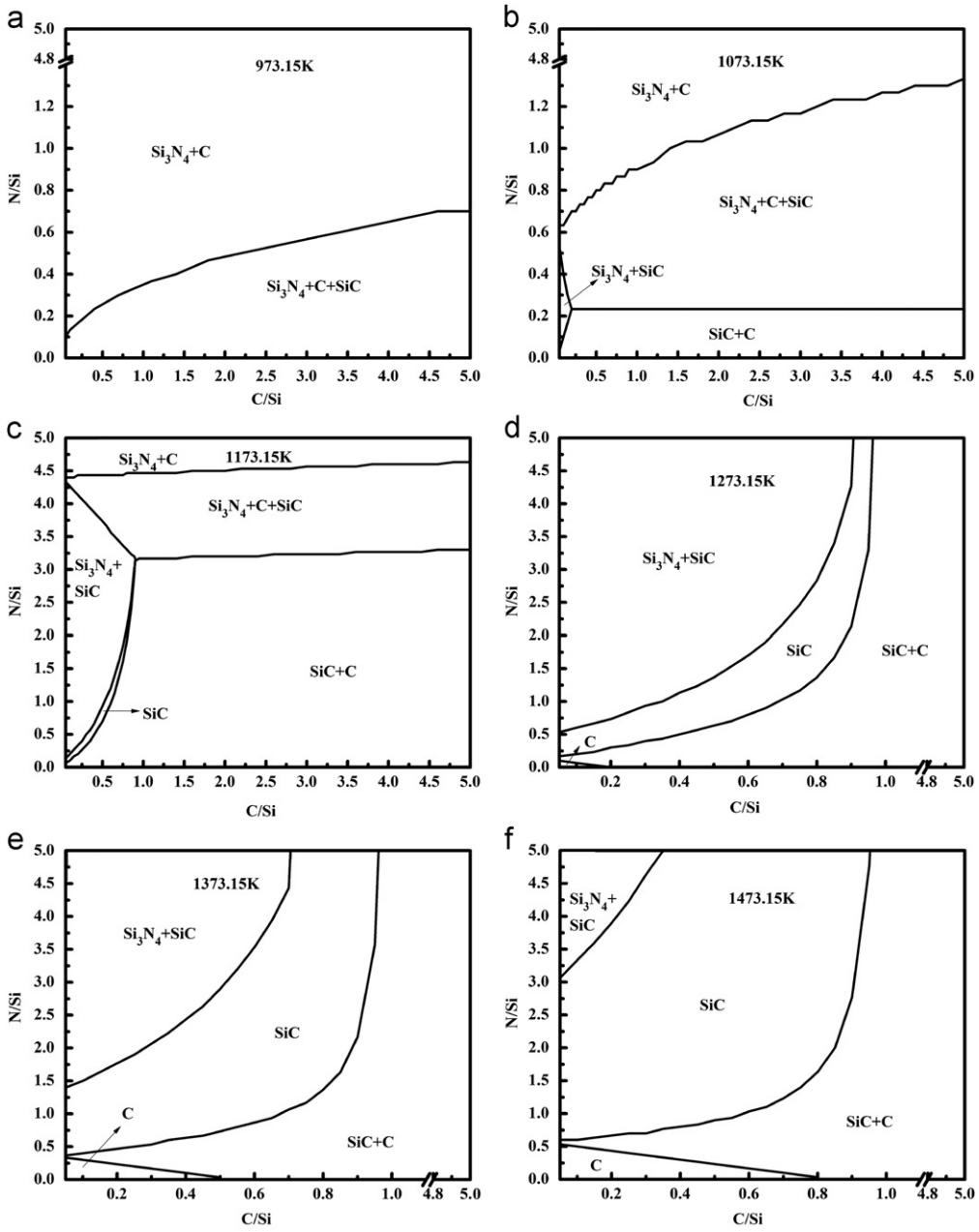

Fig. 1. The thermodynamic phase diagram from 973.15 K to 1473.15 K $[H_2]$:$[SiCl_4]=0$; $P_{Total}=0.01$ atm; $[SiCl_4]=3$ mol; (a) $T=973.15$ K; (b) $T=1073.15$ K; (c) $T=1173.15$ K; (d) $T=1273.15$ K; (e) $T=1373.15$ K and (f) $T=1473.15$ K).

When $J_P < K^{\Phi}$, $A > 0$, reaction can be carried out spontaneously.
$J_P = K^{\Phi}$, $A = 0$, reaction achieves balance.
$J_P > K^{\Phi}$, $A < 0$, reaction could not be carried out (reverse reaction itself is possible to carry out).

The effect of H_2 in the reaction system is dilution. The main chemical reactions are as follows:

$$3SiCl_4 + 4NH_3 = Si_3N_4 + 12HCl, \quad \Delta G = -380566.5\ \text{J} \quad (5)$$

$$3SiCl_4 + 3H_2 + C_3H_6 = 3SiC + 12HCl, \quad \Delta G = -41667.7\ \text{J} \quad (6)$$

$$C_3H_6 = 3C + 3H_2, \quad \Delta G = -236828.6 \quad (7)$$

$$NH_3 = N_2 + 3H_2, \quad \Delta G = -164180.2 \quad (8)$$

and the ΔG number of the chemical reactions is from Factsage database. With the increasing of H_2, Eq. (8) is restrained and then the amount of NH_3 is increasing which leads to the deposition of Si_3N_4. About the deposition of SiC, there are little extra gaseous decomposition products because 1173.15 K is much higher than the decomposition

temperature of C_3H_6, so the dissolved gas of H_2 has nothing to do with depositing SiC. So more dissolved gas of H_2 is better in order to achieve Si–C–N. But the ratio of H_2 has a negligible effect on depositing Si_3N_4 when the dilution ratio of H_2:$SiCl_4$ exceeds 10:1. Consequently H_2:$SiCl_4$=10:1 is the best dilution ratio.

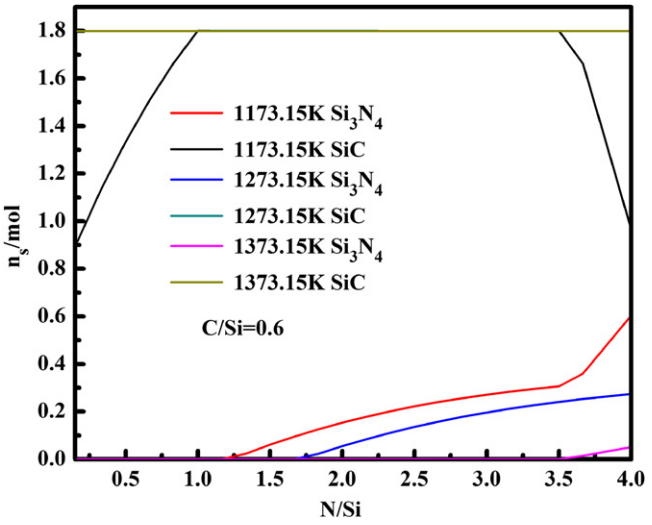

Fig. 2. Yield map of SiC–Si_3N_4 from 1173.15 K to 1373.15 K [H_2]:[$SiCl_4$]=0; P_{Total}=0.01 atm; [$SiCl_4$]=3 mol; C/Si=0.6).

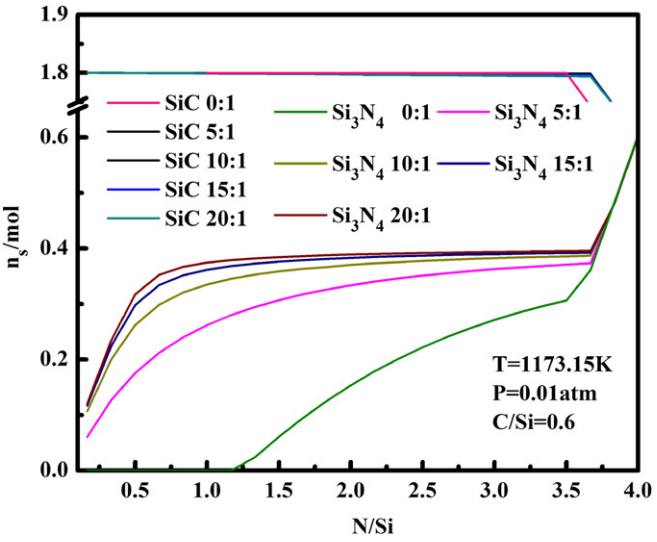

Fig. 4. Yield map with different dilution ratio of H_2 (T=1173.15 K; P_{Total}=0.01 atm; [$SiCl_4$]=3 mol; C/Si=0.6).

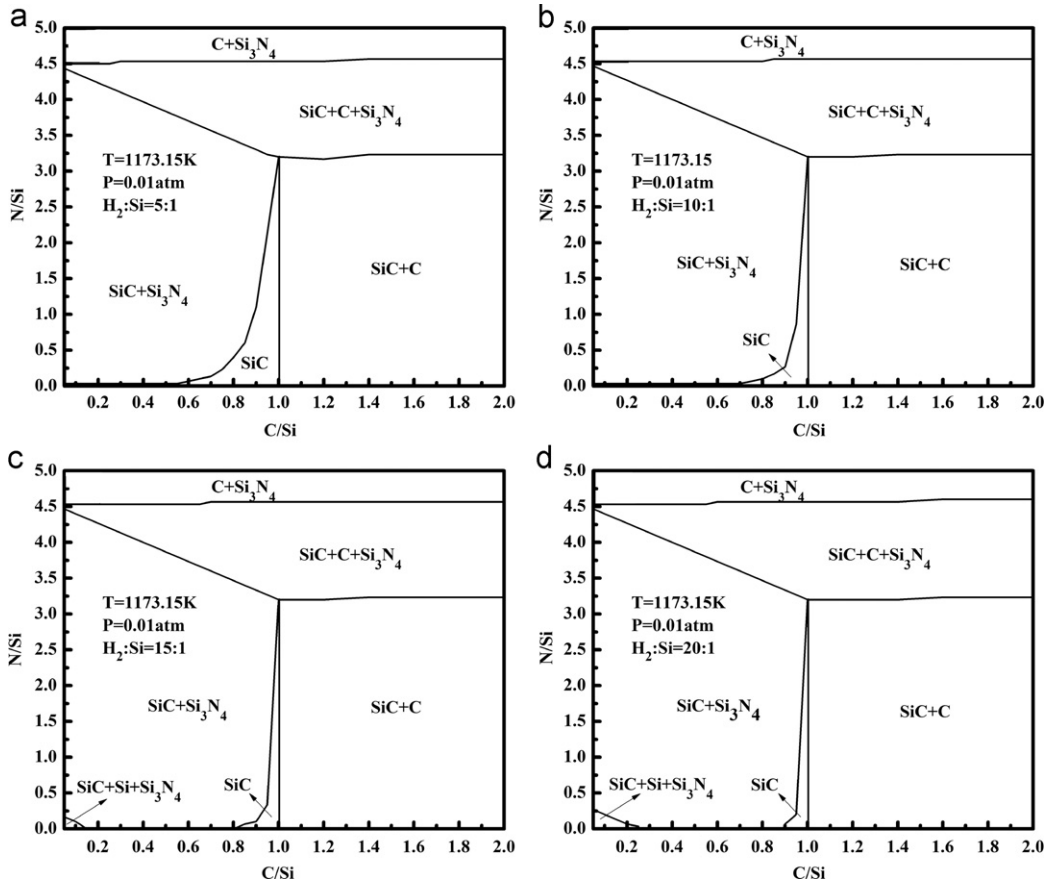

Fig. 3. The thermodynamic phase diagram with different dilution ratio of H_2 (T=1173.15 K; P_{Total}=0.01 atm; [$SiCl_4$]=3 mol; (a) [H_2]:[$SiCl_4$]=5:1; (b) [H_2]:[$SiCl_4$]=10:1; (c) [H_2]:[$SiCl_4$]=15:1 and (d) [H_2]:[$SiCl_4$]=20:1).

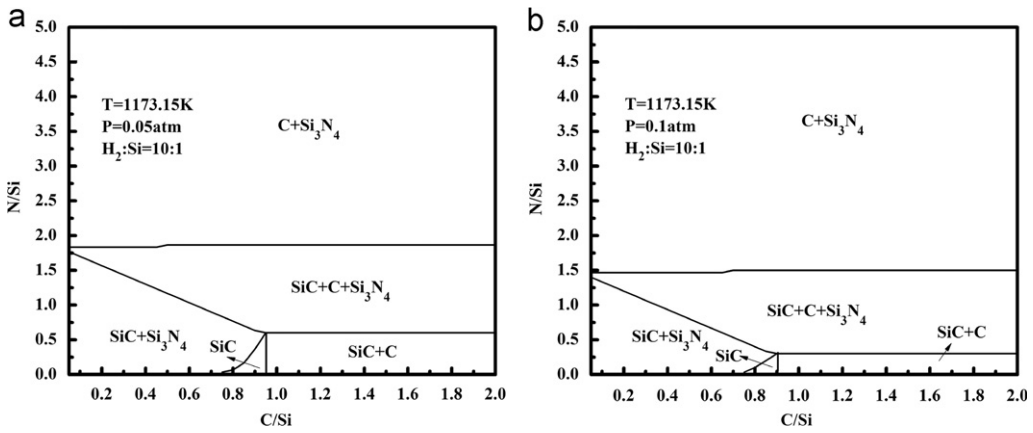

Fig. 5. The thermodynamic phase diagram with different total pressure (T=1173.15 K; [H_2]:[$SiCl_4$]=10:1; [$SiCl_4$]=3 mol; (a) P_{Total}=0.05 atm; (b) P_{Total}=0.1 atm).

3.3. The effect of total pressure on the thermodynamic phase diagram and reaction product

Fig. 5 shows the thermodynamic phase diagram with different total pressures which are 0.05 atm and 0.1 atm at 1173.15 K. Fig. 6 shows the yield map of SiC–Si_3N_4 with different total pressure when C/Si=0.8. Total pressure plays an important role in both of the formation and the yield of SiC–Si_3N_4 compared with Fig. 3b. The detailed discussions are as follows from Figs. 5 and 6:

(1) For C–Si_3N_4 and SiC–Si_3N_4, with the increasing of the total pressure from 0.01 atm to 0.1 atm, the area of C–Si_3N_4 increases and SiC–Si_3N_4 decreases accordingly. Lower total pressure makes for the deposition of double phase of SiC–Si_3N_4.
(2) For other phases, the area of other phases decreases with the increasing of the area for SiC–Si_3N_4.

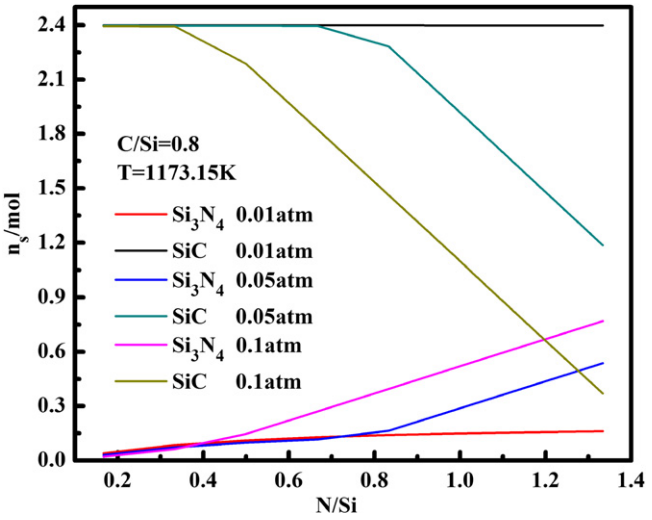

Fig. 6. Yield map with different total pressure (T=1173.15 K; [H_2]:[$SiCl_4$]=10:1; [$SiCl_4$]=3 mol; C/Si=0.8).

According to the physical chemistry theory, at a certain temperature, K^{Φ} has a fixed value. When the system pressure increases, the K^{Φ} will decrease, which means the reaction equilibrium moves toward the reactants. Therefore, as the moles of gases increase, the volume will increase at a definite temperature and pressure [19]. So increasing the system pressure will result in a balance to the volume shrinking direction. And the decomposition reaction is so complicated that the intermediate reaction cannot be deduced correctly. Nevertheless overall reaction equation and Gibbs free energy can be considered as Eqs. (5)–(7) at this temperature.

The expansion value of these Eqs. (5)–(6) is the same (in volume, the same below), which is caused by the increase of total pressure respectively. So the two reactions are restrained, but the ΔG of Eq. (5) is much smaller than that of Eq. (6). That means Eq. (5) is achieved easier than Eq. (6). Because 1173.15 K is much higher than the decomposition temperature of C_3H_6, so Eq. (7) is conducted thoroughly whatever the total pressure changes.

4. Experimental

The Si_3N_4 ceramic with high porosity fabricated in our previous work [20] was machined into specimens with dimensions of 2.16 mm × 10.16 mm × 22.86 mm and then placed into a vertical CVD furnace to deposit Si–C–N using the $SiCl_4$–NH_3–C_3H_6–H_2–Ar system. In this system, Silicon tetrachloride ($SiCl_4 \geq 99.99$ wt%) was used as Si source; propylene ($C_3H_6 \geq 99.99\%$) was C source; ammonia ($NH_3 \geq 99.99\%$) was N source; hydrogen ($H_2 \geq 99.99\%$) was the carrier gas of $SiCl_4$ and dilution gas; argon ($Ar \geq 99.9\%$) was the dilution gas. The processing conditions were T=1273.15 K, P= −0.098 MPa, C/Si=1.06, N/Si=0.59.

Fig. 7(a) showed the surface morphology of CVD Si–C–N on the Si_3N_4 substrate. As the SEM (S-2700, Hitachi, Japan) micrographs revealed, the deposition of Si–C–N ceramic was in a continuous and cauliflower-like appearance. Fig. 7(b) showed the energy dispersive spectroscopy (EDS) pattern of the deposition surface of the CVD Si–C–

N (Si:C:N=1.7:1.8:1). This result showed that the obtained film consisted of four elements, namely, Si, C, N and O. And O was probably from surface adsorption and the content was extremely low.

Fig. 8(a) showed the X-ray photoelectron spectroscopy (XPS, K-Alpha; Thermo Scientific) survey spectrum.

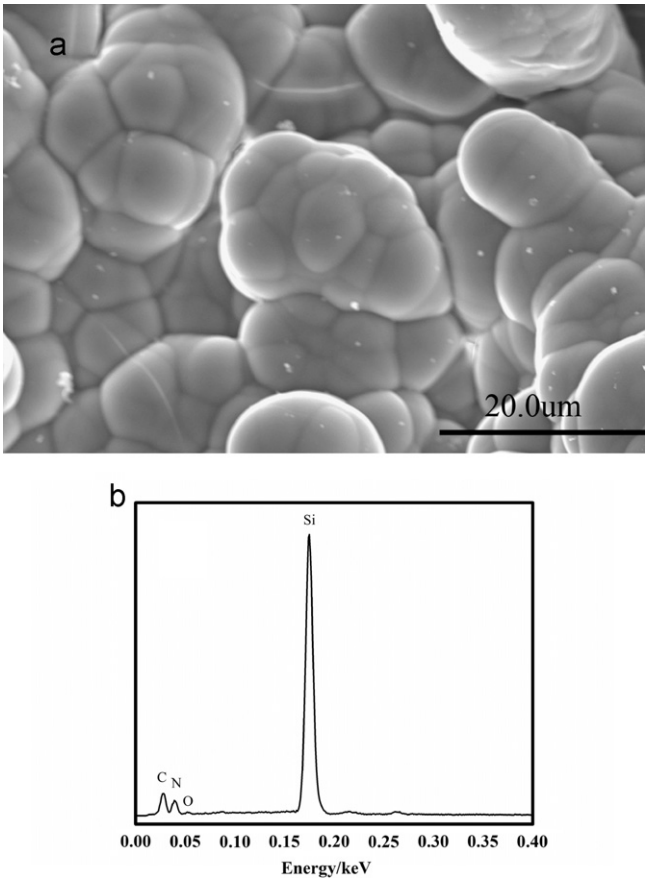

Fig. 7. (a) Scanning electronic microscopy photographs of the surface morphology of CVD Si–C–N on the Si_3N_4 substrate and (b) Energy dispersive spectroscopy pattern of the deposition surface of the CVD Si–C–N (Si:C:N=1.7:1.8:1).

Elemental composition was also measured. It was found that the obtained film was composed of Si, C, N and O. This agreed well with the results of EDS. Considering the low content of oxygen, oxygen content could be ignored. Weight change and elemental composition are shown by Table 1. And decomposition of Si (2p) was performed after fixing the binding energy difference of these peaks. Fig. 8(b) showed the high resolution XPS spectra of Si2p core levels of the obtained film. It could be found that the obtained film was predominantly constituted by Si–N and Si–C bonds. And it was clear that Si–N bonds were dominant in the obtained film.

After analysis, what could be confirmed was that the obtained Si–C–N was amorphous. In order to observe the phase composition of obtained film, the Si_3N_4–Si–C–N ceramics were heat-treated at 1773.15 K in N_2 for 2 h. Fig. 9 shows X-ray diffraction (XRD, X'Pert Pro, Philip) patterns of porous Si_3N_4 ceramics before and after CVD Si–C–N: (a) porous Si_3N_4 ceramics; (b) Si_3N_4 ceramic after CVD Si–C–N (Si:C:N=1.7:1.8:1) and heat-treated at 1773.15 K for 2 h in N_2. The main phases of the obtained Si–C–N were α-Si_3N_4 and β-Si_3N_4. The Si_3N_4 ceramic substrate was prepared by sintering at 2073 K in N_2, and when heat-treated at 1773 K in N_2, there was no α-Si_3N_4 formed. It inferred that α-Si_3N_4 was from the obtained Si–C–N film. Besides the α-Si_3N_4, amorphous Si–C–N and SiC nano-crystal may also exist in the obtained product. But those contents were so low that there were no peaks of SiC. This result was consistent with the analysis of XPS.

It can be sure that Si–C–N could be obtained by low-pressure CVD and the obtained Si–C–N was amorphous which was different from the consequences of Factsage. Nonetheless the deposition product could be transferred to α-Si_3N_4 and SiC nano-crystal which meant the product met the original intention of the design. Although this verdict had differences with the consequence of the thermodynamic calculations, the influence of deposition parameters known by thermodynamic calculations was also beneficial to the following experiments.

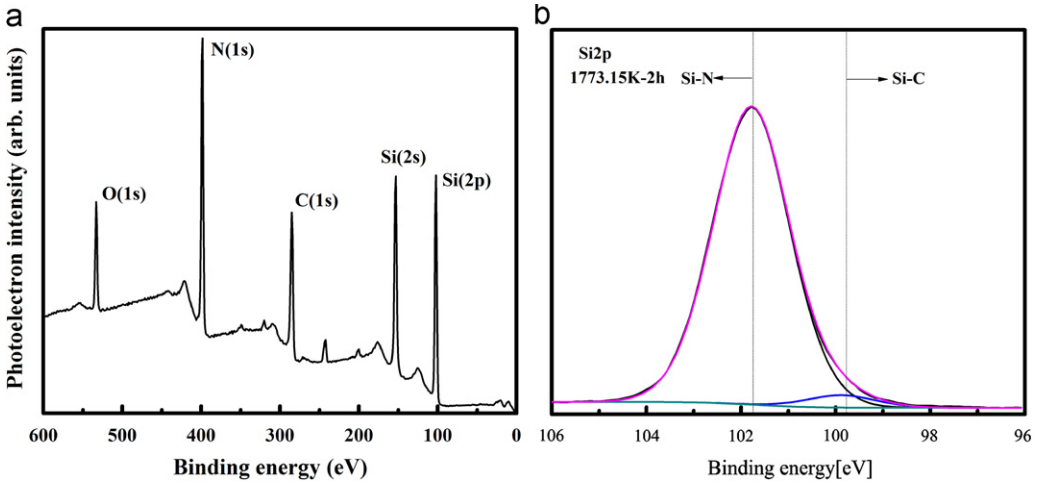

Fig. 8. (a) X-ray photoelectron spectroscopy survey spectrum and (b) High resolution XPS spectra of Si2p core levels.

Table 1
Weight change and elemental composition measured by XPS.

No.	Weight change (%)	Si (at%)	C (at%)	N (at%)
SiCN	2.44	41.1	25.7	33.2

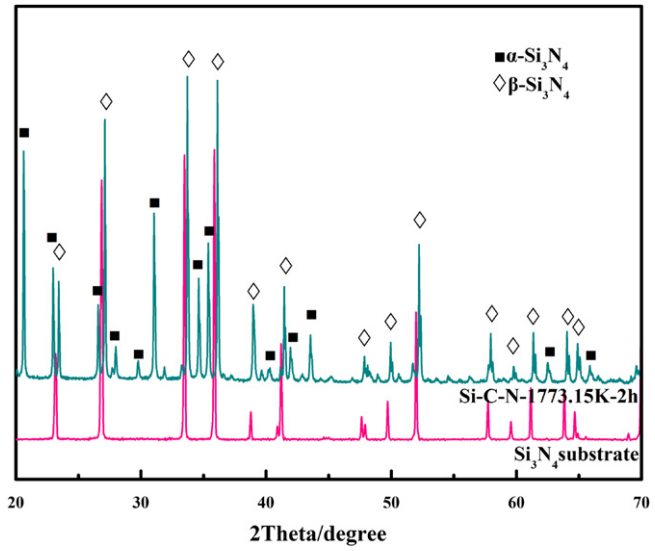

Fig. 9. X-ray diffraction patterns of porous Si_3N_4 ceramics before and after CVD Si–C–N: (a) porous Si_3N_4 ceramics; (b) Si_3N_4 ceramic after CVD Si–C–N (Si:C:N = 1.7:1.8:1) and heat-treated at 1773.15 K for 2 h in N_2.

5. Conclusions

(1) The area of SiC–Si_3N_4 increases firstly and then decreases with the rising of temperature and reaches the maximum value at 1273.15 K.
(2) The ratio of C/Si is the main factor for the deposition of SiC from the double phase of SiC–Si_3N_4.
(3) $T = 1173.15$ K, H_2:$SiCl_4 = 10:1$, and $P_{Total} = 0.01$ atm make for the deposition of Si_3N_4. Taking the deposition of SiC into consideration, the deposition of Si_3N_4 influences the formation of Si–C–N directly.
(4) According to the influencing factors of depositing SiC and Si_3N_4, the suitable parameter for deposition of Si–C–N can be determined.
(5) Through the experimental verification, it can be demonstrated that Si–C–N can be obtained by low-pressure CVD, its product being amorphous and principally constituted by Si–N and Si–C bonds. The obtained Si–C–N ceramics can transform to α-Si_3N_4 and SiC nanocrystal when heat-treated at 1773.15 K in N_2 for 2 h.

Acknowledgments

The authors acknowledge the support of the Chinese National Foundation for Natural Sciences under Contracts (Nos. 51002120 and 51032006). Project was supported by the Research Fund of State Key Laboratory of Transient Optics and Photonics, Chinese Academy of Sciences, China (Grant no. SKLST201106).

References

[1] H. Morkoc, S. Strite, G.B. Gao, M.E. Lin, B. Sverdlov, M. Buens, Large-band-gap SiC, III–V nitride, and II–VI ZnSe-based semiconductor device technologies, Journal of Applied Physics 76 (1994) 1363–1384.
[2] P.A. Ivanov, V.E. Chelnokov, Recent developments in SiC single-crystal electronics, Semiconductor Science and Technology 7 (1992) 863–880.
[3] H.L. Chang, C.T. Kou, Characteristics of Si–C–N films deposited by microwave plasma CVD on Si wafers with various buffer layer materials, Diamond and Related Materials 10 (2001) 1910–1915.
[4] K.B. Sundaram, J. Alizadeh, Deposition and optical studies of silicon carbide nitride thin films, Thin Solid Films 370 (2000) 151–154.
[5] P. Bohacek, J. Huran, A.P. Kobzev, N.I. Balalykin, J. Pezoltd, PECVD Silicon Carbon Nitride Thin Films: Properties, in: Proceedings of the Seventh International Conference on Advanced Semiconductor Devices and Microsystems, 2008, pp. 191–194.
[6] W. Cheg, J. Jiang, Y. Zhang, H. Zhu, D. Shen, Effect of the deposition conditions on the morphology and bonding structure of SiCN films, Materials Chemistry and Physics 85 (2004) 370–376.
[7] R. Riedel, H.-J. Kleebe, H. Schonfelder, F. Aldinger, A covalent micro-/nano-composite resistant to high-temperature oxidation, Nature 374 (1995) 526–528.
[8] A. Bendeddouche, R. Berjoan, E. Beche, R. Hillel, Hardness and stiffness of amorphous SiC_xN_y chemical vapor deposited coatings, Surface Coatings and Technology 111 (1999) 184–190.
[9] Akira Izumi, Koshi Oda, Deposition of SiCN films using organic liquid materials by HWCVD method, Thin Solid Films 501 (2006) 195–197.
[10] G. Viera, J.L. Andujar, S.N. Sharma, E. Bertran, Si–C–N nanometric powder produced in square-wave modulated RF glow discharges, Diamond and Related Materials 7 (1998) 407–411.
[11] P. Jedrzejowski, J. Cizek, A. Amassian, J.E. Klemberg-Sapieha, J. Vlcek, L. Martinu, Mechanical and optical properties of hard SiCN coatings prepared by PECVD, Thin Solid Films 447–448 (2004) 201–207.
[12] J.-J. Wu, C.-T. Wu, Y.-C. Liao, T.-R. Lu, L.C. Chen, K.H. Chen, L.-G. Hwa, C.-T. Kuo, Deposition of silicon carbon nitride films by ion beam sputtering, Thin Solid Films 355–356 (1999) 417–422.
[13] Fa Luo, Dongmei Zhu, Hua Zhang, Wancheng Zhou, Dielectric and mechanical properties of hot-pressed SiCN/Si_3N_4 composites, Journal of Electroceramics 17 (2006) 83–86.
[14] Xueming Li, Size Yang, Xingfang Wu, Preparation of silicon carbide nitride films on Si substrate by pulsed high-energy density plasma, Journal of Environmental Science and Technology 13 (2006) 272–276.
[15] T. Nishimura, R. Haug, J. Bill, Mechanical and thermal properties of Si–C–N material from polyvinylsilazane, Journal of Materials Science. 33 (1988) 237–5241.
[16] Guifang Han, Fundamental manufacturing techniques by CVI route for continuous fiber reinforced silicon nitride matrix composites, College of Materials Science and Engineering NPU Doctoral Dissertation, 2008 pp. 27–33.
[17] Y. Ohzawa, H. Hoshino, M. Fujikawa, K. Nakane, K. Sugiyama, Preparation of high-temperature filter by pressure-pulsed chemical vapor infiltration of SiC into carbonized paper-fiber performs, Journal of Materials Science 33 (1998) 5259–5264.
[18] S. Song, G. Zhuang, Z. Wang, Higher Education Press, 1995, pp. 271–275.
[19] Yongsheng Liu, Shanhua Liu, Xinzhang Zuo, Research on stability diagrams for BCl_3–C_3H_6–H_2 system, Journal of Chinese Ceramics Society 38 (2010) 183–187.
[20] X.W. Yin, X.M. Li, L.T. Zhang, Laifei Cheng, Yongsheng Liu, Tianhao Pan, Microstructure and mechanical properties of Lu_2O_3-doped porous silicon nitride ceramics using phenolic resin as pore-forming agent, Applied Ceramics Technology 7 (2010) 391–399.